A Quantum Mechanical Study of the Decomposition of CF_3OCF_3 and $CF_3CF_2OCF_2CF_3$ in the Presence of AlF_3

Bangwu Jiang, David J. Keffer,* and Brian J. Edwards

Department of Chemical and Biomolecular Engineering, University of Tennessee, Knoxville, Tennessee 37996-2200

Received: August 24, 2007; In Final Form: January 4, 2008

The effect of AlF_3 on the decomposition of CF_3OCF_3 and $CF_3CF_2OCF_2CF_3$ is investigated using ab initio theory. Previous work by Pancansky et al. [Pacansky, J.; Waltman, R. J. *J Fluorine Chem.* **1997**, *83*, 41] showed that AlF_3 significantly reduces the activation energy of the decomposition of CF_3OCF_3 due to the strong electrostatic interaction between the aluminum trifluoride and the reactant. In this work, a new transition-state structure and reaction mechanism have been identified for the decomposition of CF_3OCF_3 in the presence of AlF_3. This new mechanism shows that AlF_3 functions by accepting a fluorine atom from one carbon and simultaneously donating a fluorine atom to the other carbon. We show that the same pathway is obtained independently of the level of theory. The reaction rate, generated via statistical mechanics and transition-state theory, is 2−3 orders of magnitude higher for the new transition state when compared to that of the old one. The study was also performed for $CF_3CF_2OCF_2CF_3$ in order to ascertain the effect of chain length on the reaction mechanism and rate. We find that an analogous transition state, with lower activation energy, provides the lowest-energy path for decomposition of the longer chain.

1. Introduction

Perfluoropolyethers (PFPEs) are lubricants used in a range of diverse technologies, such as computer drives, diffusion pumps, and high-performance turbine jet engines, due to their generally excellent thermal and chemical stabilities.[1−3] While the strong C−F bond makes PFPE molecules more resistant to thermal breakdown than alkyl ethers, PFPE molecules degrade readily under certain conditions, such as irradiation and high temperature in the presence of metal surfaces.[4−6]

The decomposition of perfluoropolyethers (PFPEs) was investigated by Pacansky et al. through ab initio theory for the model molecule prefluorodimethyl ether (PFDME), CF_3OCF_3, with and without the existence of a metal surface of AlF_3.[7,8] Another model molecule, $CF_3CF_2OCF_2CF_3$, was studied by Waltman.[9] It was concluded that at the high levels of theory, the thermal decomposition of CF_3OCF_3 is exothermic. The reaction path involving a "cyclic" transition state (TS1) (shown in the Figure 1) is favorable over the direct C−O free-radical bond scission without the presence of AlF_3. In the presence of AlF_3, the activation energy for the decomposition of CF_3OCF_3 decreases approximately from 420 to 210 kJ/mol, showing a significant catalytic effect.

In this work, we examine again the catalytic effect of AlF_3 on the decomposition of CF_3OCF_3 and $CF_3CF_2OCF_2CF_3$. A new transition state (TS2) with a lower energy is identified through the same level of theory, which shows that AlF_3 functions as the carrier of fluorine atoms in the transition state. The new transition state for PFDME is shown in Figure 1, demonstrating that the aluminum atom in AlF_3 interacts strongly with the oxygen atom in PFDME. Meanwhile, one of the fluorine atoms in AlF_3 moves to one carbon atom to form CF_4, and one of the fluorine atoms of the other carbon atom leaves, thus producing

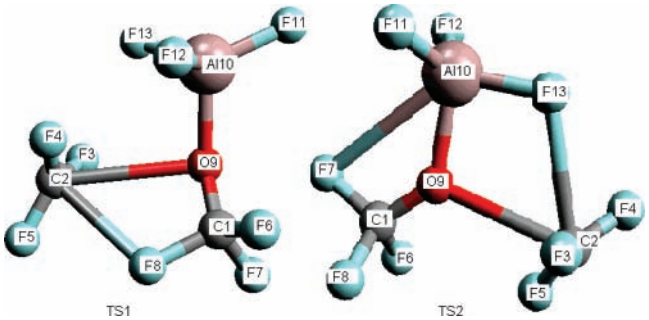

Figure 1. The optimized geometries for the transitions TS of PFDME−AlF_3 computed through the B3LYP 6-31G* basis set. The right illustration was obtained according to the proposal of Pacansky et. al;[7] the left illustration is the revision proposed in this work.

COF_2·AlF_3. Optimized structures of PFDME and PFDME−AlF_3 are shown in Figure 2. The elementary steps involved in the decomposition of PFDME in the presence of AlF_3 are as follows

$$CF_3OCF_3 + AlF_3 \xrightarrow{I} CF_3OCF_3\cdot AlF_3 \xrightarrow{II} TS1(TS2) \xrightarrow{III} CF_4 + COF_2\cdot AlF_3 \xrightarrow{IV} CF_4 + COF_2 + AlF_3$$

The energy differences in the elementary steps I, II, III, and IV calculated by B3LYP[10−14] with the 6-31G*[15] basis are plotted in Figure 3, which shows that both CF_3OCF_3·AlF_3 and COF_2·AlF_3 complexes are very stable. In reality, AlF_3 intends to stay with the compounds with oxygen (CF_3OCF_3 and COF_2) to form a complex. In particular, for COF_2·AlF_3, the Lewis acid, AlF_3, has a very strong interaction with the C=O group. For the purpose of investigating the decomposition of CF_3OCF_3, we focus on step II.

2. Computational Method

Ab initio calculations were performed using Gaussian 98.[16] Pacansky et al.[7,8] performed their ab initio calculations using

* To whom correspondence should be addressed. E-mail: dkeffer@utk.edu.

10.1021/jp0768017 CCC: $40.75
Published on Web 02/16/2008

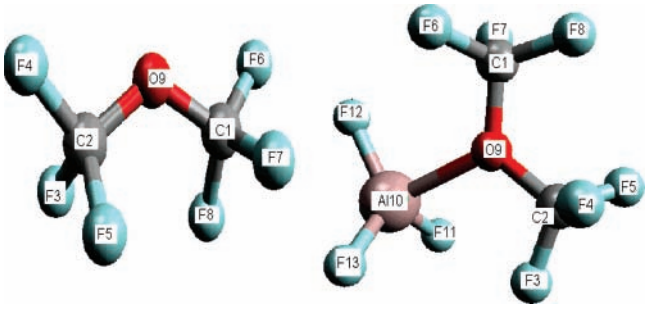

Figure 2. The optimized geometries of PFDME (left) and PFDME−AlF_3 (right) computed through the B3LYP 6-31G* basis set.

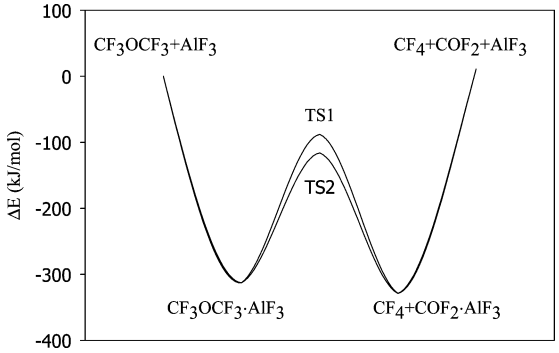

Figure 3. The energy difference in the reaction computed through B3LYP 6-31G*.

the Mulliken computer code.[17] We have repeated the calculation of the geometry optimization and energy with Gaussian 98[16] using the same level of theory, Hartree−Fock (HF) theory with the 6-31G* basis set,[15] and find that all of the results are essentially the same in the case of their transition state, TS1. In this work, we will not include any data from the theory level HF 6-31G* because it is of comparatively low level now due to the increase of computational power.

We applied the hybrid density functional B3LYP[10−14] methods with the 6-31G*[15] and 6-311G* basis sets to investigate the same transient state (TS1) as that proposed by Pacansky et al. (TS1) and located a new transient state (TS2) with appreciably lower energy in this paper. We performed the calculation with two different levels of theory in order to make sure that the relative energetic difference is not due to differing levels of accuracy.

Quantum mechanical methods and transition-state theory[18] can be applied to estimate the rate constants of the elementary reaction through the calculation of the vibration frequencies of the transition state through the ideal polyatomic gas model of statistical mechanics.[19] According to transition-state theory, the rate constant of an elementary reaction can be estimated according to the following formula[18,20]

$$k = \kappa(T)\left(\frac{P_0}{RT_0}\right)^{-m}(k_B T/h)\exp(-\Delta G_0/RT) \qquad (1)$$

where $\kappa(T)$is the tunneling correction term, k_B is the Boltzmann constant, T_0 and P_0 are the temperature and pressure references, respectively, m is the change in the number of molecules from reactants to the transition state, h is Planck's constant, R is the ideal gas constant, T is the absolute temperature, and ΔG_0 is the change of the Gibbs free energy from reactants to the transition state. The Gibbs free energy change is expressed as

$$\Delta G_0 = \Delta H_0 - T\Delta S_0 \qquad (2)$$

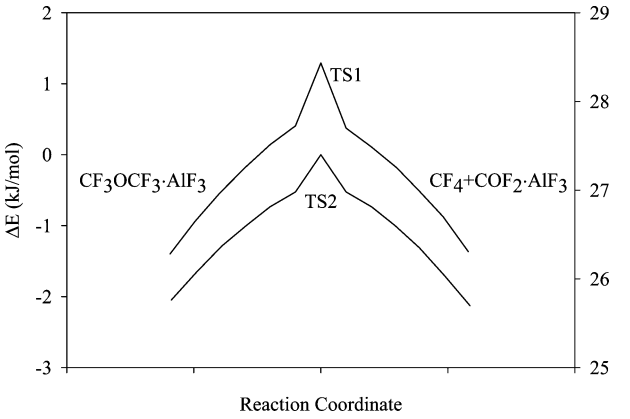

Figure 4. The energy difference along the reaction coordinate computed through B3LYP 6-31G*. All of the data are relative to the energy of TS2. (ΔE for TS2 is expressed on the secondary y axis.)

where ΔH_0 and ΔS_0 are the changes of enthalpy and entropy from reactant to the transition state, respectively. They are estimated through the ideal polyatomic gas model in statistical mechanics.[19] The scaling factors of 0.9806 and 0.989 were applied to correct the thermal energies (including zero-point energy) for B3LYP 6-31G* and B3LYP 6-311G, respectively.[21−23]

We use the Wigner tunneling expression as follows to account for the tunneling contribution to the rate constant involving the transition state

$$\kappa(T) = 1 + \frac{1}{24}\left(\frac{h\nu_s}{k_B T}\right)^2 \qquad (3)$$

where ν_s is the imaginary frequency in the transition state.

The vibrational mode with the lowest frequency in both the ground state and transition state was treated as internal rotation, calculated by assuming the torsional potential to have the simple form $U(\phi) = V[1 - \cos(\sigma_{\{int\}}\phi)]^2$, using the tables in ref 24, where $\sigma_{\{int\}}$ is the internal symmetry number and V is the torsion barrier. The remainder of the vibrational modes were treated harmonically. Although the transition state defined by the free energy is known to vary with temperature and pressure, the effect is generally slight.[20,25] In this work, our intention is to compare the rate constant between two reaction mechanisms; therefore, we do not consider the slight temperature dependence of the transition-state structures.

3. Results and Discussion

3.1. Two Reaction Mechanisms. The formation of TS1 for compound C_2F_6O under the existence of AlF_3 shown in Figure 1 has been elaborated by Pacansky et al.[7] through HF 6-31G*. We reinvestigate it through two different theory levels, B3LYP 6-31G* and B3LYP 6-311G*. In Figure 4, the energy variation along the reaction coordinate proved the validity of TS1 and TS2; the energy decreases on both sides of identified transition-state structures. In TS1, the strong electrostatic interaction between the aluminum substrate and the CF_3OCF_3 ether oxygen atom stabilizes the transition state. In order to form the products CF_4 and COF_2, one fluorine atom must be transferred from C1 to C2. The information on the angles and dihedrals is given in the Supporting Information. The following discussion is based on the results obtained through the B3LYP 6-31 G* theory level. In TS1, this fluorine atom transfer from C1 to C2 is realized mainly through decreasing the C1O9C2 bending angle from 121 to 96°. The fluoride affinity of AlF_3 is quite high, which means

TABLE 1: Energy of Compounds Calculated through B3LYP 6-31G* without the Correction for the Zero-Point Energy Calculated from Quantum Mechanics. Note: C_2 Refers to C_2F_6O and C_4 Refers to $C_4F_{10}O$. Energy Differences Are Only Calculated between $C_2 \cdot AlF_3$ and the TS at the Same Theoretical Level

compound	energy (hartrees)	difference (kJ/mol)
AlF_3	−542.072946	
C_2	−750.488388	
COF_2	−313.007945	
CF_4	−437.476256	
$COF_2 \cdot AlF_3$	−855.210490	
C2·AlF3	−1292.680583	313
TS (ref)	−1292.594928	225
TS (new)	−1292.605659	197
C4·AlF3	−1768.235074	
C4_TS (ref)	−1768.157074	205
C4_TS (new)	−1768.166566	180

TABLE 2: Optimized Bond Distance (Å) of Compounds Calculated by B3LYP 6-31 G* and B3LYP 6-311G* (marked by *)

parameters	C2−AlF3	C2−AlF3*	TS1	TS1*	TS2	TS2*
C1−O9	1.434	1.441	1.296	1.283	1.331	1.314
C2−O9	1.423	1.429	2.623	2.644	2.364	2.490
Al10−O9	2.108	2.166	1.865	1.847	1.833	1.831
C1−F6	1.317	1.316	1.340	1.346	1.357	1.362
C1−F7	1.317	1.314	1.344	1.342	1.347	1.347
C1−F8	1.328	1.325	1.433	1.438	1.350	1.365
C2−F3	1.320	1.316	1.247	1.234	1.260	1.244
C2−F4	1.323	1.323	1.244	1.235	1.268	1.249
C2−F5	1.323	1.322	1.261	1.252	1.272	1.254
Al10−F11	1.650	1.668	1.658	1.847	1.656	1.679
Al10−F12	1.654	1.669	1.673	1.684	1.657	1.678
Al10−F13	1.650	1.668	1.685	1.716	1.726	1.739
F8−C2	2.609	2.618	2.379	2.496	3.660	3.544
F13−C2	3.400	3.427	2.983	3.024	2.239	2.289
F7−Al10	3.322	3.348	3.947	3.481	3.037	3.166

that the fluorine atom can easily attach to AlF_3. Therefore, it is highly probable that AlF_3 acts as a carrier of the fluorine atom from C1 to C2. The proposed transition state of TS2, shown in Figure 1, is based on this assumption. If TS2 has a lower energy level than TS1, then TS2 is more favorable than TS1 in the decomposition of PFDME in the presence of AlF_3. The data in Table 1 prove this point and show that the energy difference (corresponding to the activation energy) between $CF_3OCF_3-AlF_3$ in TS2 is about 10% lower than that in TS1 at both theory levels of theoretical treatment, B3LYP 6-31G*. Similar results appear through B3LYP 6-311G*.

3.2. Geometric Change and Partial Charge Distribution between Transition States. The optimized parameters of the bond lengths are collected in Table 2. The detailed information on the angle can be found in Supporting Information. Since the main geometrical changes are similar between the two theory levels, we will focus on the results from B3LYP 6-31G*. The strong interaction between AlF_3 and CF_3OCF_3 is observed through comparison of the optimized structures of $CF_3OCF_3-AlF_3$ and CF_3OCF_3, which was well stated by Pacansky et al.[7] As for the transition-state structure, the notable structure difference between TS1 and TS2 is that C1O9C2 angles in TS1 and TS2 are about 96 and 127°, respectively, compared to 121° in $CF_3OCF_3-AlF_3$, which means that in order to transfer the fluorine atom between C1 and C2, C1O9C2 angles in TS1 need to decrease about 25°. On the other hand, C1O9C2 angles in TS2 need to increase by only about 6°. The C1O9C2 bending angle in $CF_3OCF_3-AlF_3$ is almost the same as that in CF_3OCF_3, demonstrating that the interaction between CF_3OCF_3 and AlF_3 neither increases nor decreases the C1O9C2 angle. Therefore, it is not necessary to have a huge bending angle change in the transition state of this reaction. Moreover, there are larger changes in both CO bond distances in TS1 than in TS2. The compressed bond of C1O9 in TS1 is 0.02 Å shorter than that in TS2. The elongated bond of C2O9 in TS1 is 0.02 Å longer than that in TS2. It is noteworthy that the interaction between CF_3OCF_3 and AlF_3 shown in the optimized $CF_3OCF_3-AlF_3$ structure will increase both CO bonds by about 0.04 Å.

Since the reaction mechanism is governing the transfer of fluorine, we can also examine those distances. In TS1, in which F8 is being transferred from C1 to C2, the C1F8 bond distance changes from 1.30 to 1.38 Å, and the C2F8 separation decreases from 2.57 to 2.50 Å. In TS2, in which F7 is being transferred from C1 to Al10, the C1F7 bond distance increases from 1.29 to 1.32 Å, and the Al10F7 separation decreases from 3.32 to 3.03 Å. Also in TS2, in which the F13 is being transferred from Al10 to C2, the Al10F13 bond distance increases from 1.63 to 1.70 Å, and the C2F13 separation decreases from 3.39 to 2.45 Å. The change of the C2F13 separation in TS2 is the most striking, but this change is a nonbonded distance, which is comparably easier to change than a covalent bond length. Moreover, a 0.4 Å decrease of the C2F13 separation is observed even in TS1.

The atomic partial charge distribution obtained through the Mulliken and natural population analysis using B3LYP 6-31G* is shown in Table 3. As is well-known, the two methods give very different magnitudes in the charge distribution. Both Mulliken and natural population analyses show similar qualitative behavior, except that the charges of two carbons change in slightly different ways between the reactant and transient state.

On the basis of the Mulliken partial charges, in TS1, the fluorine atom F13 has 0.05 and 0.03 higher negative charge than that of F11 and F12 respectively, and the Al10F13 bond length is 0.034 and 0.018 Å longer than that in Al10F11 and

TABLE 3: The Partial Charge of Atoms in Different Compounds by the B3LYP 6-31 G*. The Symbol * Stands for the Mulliken Partial Charge; Otherwise the Data Are Obtained through Natural Population Analysis

atom	C_2	C_2*	C2−AlF3	C2−AlF3*	TS1	TS1*	TS2	TS2*
C1	1.35	0.97	1.37	1.03	1.32	0.98	1.34	1.01
C2	1.35	0.97	1.37	1.06	1.45	0.94	1.42	0.93
F3	−0.35	−0.24	−0.32	−0.21	−0.18	−0.02	−0.22	−0.07
F4	−0.34	−0.23	−0.33	−0.22	−0.18	−0.01	−0.22	−0.07
F5	−0.35	−0.25	−0.33	−0.22	−0.22	−0.07	−0.23	−0.08
F6	−0.34	−0.23	−0.32	−0.20	−0.35	−0.24	−0.38	−0.28
F7	−0.35	−0.24	−0.32	−0.20	−0.42	−0.26	−0.37	−0.25
F8	−0.35	−0.25	−0.34	−0.23	−0.36	−0.35	−0.36	−0.28
O9	−0.62	−0.51	−0.72	−0.64	−0.92	−0.64	−0.92	−0.67
Al10			1.99	1.17	1.95	1.09	1.97	1.11
F11			−0.69	−0.44	−0.68	−0.45	−0.68	−0.44
F12			−0.69	−0.44	−0.70	−0.47	−0.68	−0.45
F13			−0.69	−0.44	−0.72	−0.50	−0.65	−0.45

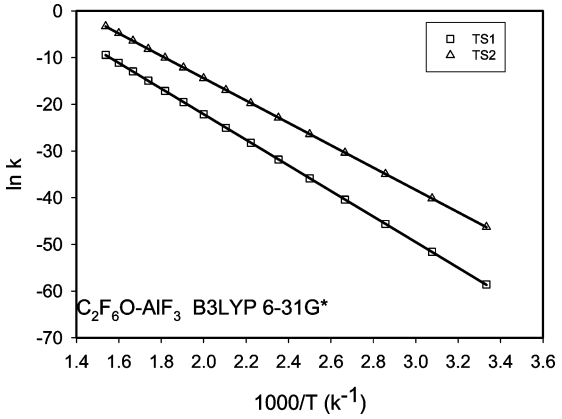

Figure 5. Arrhenius plot of the thermal rates of C_2F_6O in the presence of AlF_3 calculated using B3LYP 6-31G*.

TABLE 4: Prefactor K_0 and Activation Energy E_a of Different Reactions Pathways at Two Levels of Theory. The Symbol * Stands for Results from B3LYP 6-311G*; Otherwise the Results Are from B3LYP 6-31G*

reaction	K_0 (s^{-1})	E_a (kJ/mol)
C_2F_6O−TS1	1.6×10^{14}	228
C_2F_6O−TS2	3.5×10^{14}	199
$C_4F_{10}O$−TS1	7.9×10^{13}	197
$C_4F_{10}O$−TS2	2.4×10^{14}	172
C_2F_6O−TS1*	3.1×10^{14}	192
C_2F_6O−TS2*	6.0×10^{14}	168

Al10F12, respectively. This demonstrates that F13 is poised to leave Al10 even in TS1. Partial charges of F11 and F12 are not the same, and neither are the bond lengths of Al10F11 and Al10F12. In TS2, the fluorine atom F13 also has a 0.05 higher negative charge than that of F11 and F12, and the Al10F13 bond length is also 0.051 Å longer than that in Al10F11 and Al10F12. Therefore, the difference in TS2 is slightly higher than that in TS1; moreover, fluorine atoms F11 and F12 share the same partial charge and AlF bond length. This demonstrates that the fluorine F13 in TS2 has a much higher potential to leave Al10 than that of fluorine F13 in TS1. Partial charge distribution and the corresponding bond length change also show that fluorine atom F8 in TS1 is poised to leave C1, but in TS2, there is no clue to support the notion that the fluorine atom F8 in TS2 intends to leave C1. Consequently, from the investigation of the energy differences in Table 1, supported by geometric changes and partial charge redistribution between transition states, we have found qualitative proof that TS2 is more competitive than TS1 in the decomposition of CF_3OCF_3.

3.3. Reaction Rates for the Two Reaction Mechanisms. The reaction heat, entropy, and Gibbs free energy of the rate-limiting reaction $CF_3OCF_3 \cdot AlF_3$IITS1(TS2) were carried out using statistical mechanics[19] and transition-state theory[18] at temperatures between 300 and 650 K. Figure 5 shows Arrhenius plots for both transition states calculated with B3LYP 6-31G*. The solid lines are obtained by fitting the data obtained through statistical mechanics and transition-state theory by using the Arrhenius equation. The corresponding parameters, prefactor K_0 and activation energy E_a of different reactions pathways for different cases, are listed in Table 4. In Figure 5, we observe that the temperature dependence of the reaction rates involving both transient states follows the Arrhenius relation faithfully. The reaction rate involving TS2 is approximately 2−3 orders of magnitude higher than that of TS1 at temperatures between 300 and 650 K. From Table 4, at the B3LYP 6-31G* theory level, the activation energy, E_a, involving TS1 and TS2 is 228 and 199 kJ/mol, respectively, while the prefactor, K_0, is 1.6×10^{13} and 3.5×10^{14} s^{-1}, respectively. Both prefactors and activation energies clearly show that the reaction involving TS2 is much more favorable than the one involving TS1.

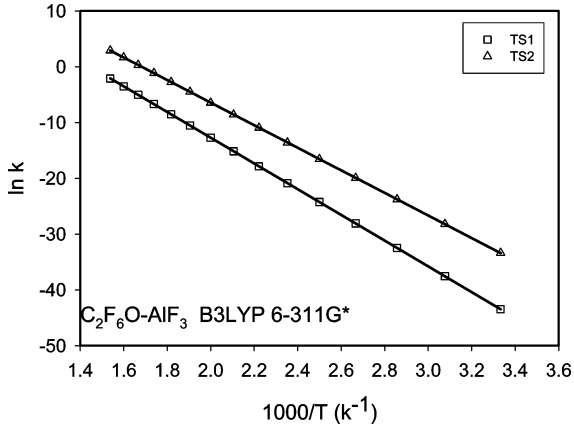

Figure 6. Arrhenius plot of the thermal rates of C_2F_6O in the presence of AlF_3 calculated using B3LYP 6-311G*.

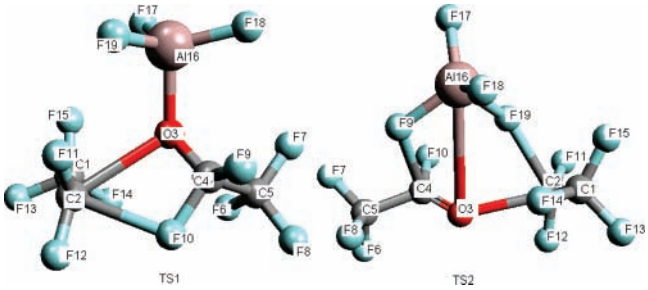

Figure 7. The optimized geometries for the transitions of $C_4F_{10}O$−AlF_3 computed through the B3LYP 6-31G* basis set. The right illustration is the transition state calculated according to Pacansky et al.[7] The left one is the revision proposed in this work.

Arrhenius plots for both transition states based on the B3LYP 6-311G* are presented in Figure 6. Similarly to Figure 5, Figure 6 demonstrates that the reaction involving TS2 has a reaction rate which is 2−3 orders of magnitude higher than that involving TS1. For the same reaction mechanism, the reaction rate predicted by B3LYP 6-311G* is approximately 2−3 orders of magnitude higher than that of B3LYP 6-31G*, mainly due to the fact that the activation energy predicted by 3LYP 6-311G* is about 30 kJ/mol lower than that of B3LYP 6-31G*. At this time, there is no experimental data available for this reaction rate to determine which level of theory is providing a better prediction.

3.4. The Effect of Chain Length. An analogous study and comparison was carried out for a longer chain perfluoroether $CF_3CF_2OCF_2CF_3$ using B3LYP 6-31G*. In this case, we do not report the detailed geometrical changes since we found a similar trend in this longer-chain compound as was found for the shorter chain. The snapshots of the two transient states of $CF_3CF_2OCF_2$-CF_3−AlF_3 are presented in Figure 7. The right transient state, TS1, is calculated according to the reference by Pacansky et al.[7] The left one, TS2, is the revision proposed in this work. There are no remarkable points of difference between TS1 for the short and long chains. However, in TS2 for $CF_3CF_2OCF_2$-CF_3, we see some stronger evidence that AlF_3 functions as a carrier of the fluorine atom from C4 to C2. The results from quantum calculations using B3LYP 6-31G* show that from the reactant to TS2, the bond length C4F9 extends from 1.475 to 2.166 Å. Also, the separation of Al16F9 decreases from 2.909 to 1.718 Å, considering that Al16F17, Al16F18, and Al16F19 in TS2 are 1.662, 1.666, and 1.750 Å. Therefore, there is a clear

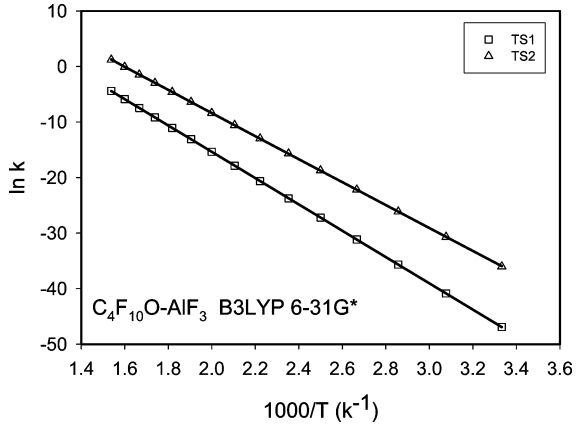

Figure 8. Arrhenius plot of the thermal rates of $C_4F_{10}O$ in the presence of AlF_3 calculated using B3LYP 6-31G*.

picture in TS2 that F9 is leaving C4 and approaching Al16. On the other hand, from the reactant to TS2, the separation of C2F19 decreases from 3.587 to 2.239 Å, and the bond length Al16F19 (1.750 Å) is even larger than the separation in Al16F9; this proves that F19 is leaving Al16 and approaching C2.

Arrhenius plots for both transition states of $CF_3CF_2OCF_2CF_3$ based on the B3LYP 6-31G* are shown in Figure 8. These also demonstrate that the reaction involving TS2 has a rate that is 2−3 orders of magnitude higher than that involving TS1. The comparison between Figures 5 and 8 shows that, at the same level of theory and for the same transition state, the reaction rate of $CF_3CF_2OCF_2CF_3$ is about 2−3 orders higher than that of CF_3OCF_3. The corresponding parameters of the Arrhenius equation are listed in Table 4, which shows that at the same theory level B3LYP 6-31G* and the same transient state, the activation energy of $CF_3CF_2OCF_2CF_3$ is approximately 28 kJ/mol lower than that of CF_3OCF_3. Table 1 shows that at B3LYP 6-31G* theory level and the same transient state, the energy barrier involving $CF_3CF_2OCF_2CF_3$ is approximately 18.4 kJ/mol lower than that involving CF_3OCF_3. From the references,[7,9] at HF 6-31G*, for TS1, the energy barrier involving $CF_3CF_2OCF_2CF_3$ is approximately 14.0 kJ/mol lower than that involving CF_3OCF_3. Several previous studies showed that the fluorine atom in CF_2 behaves differently from that in CF_3.[26−29] The bond energy of a C−F bond in a CF_2 group is much lower than that of a CF_3 group, which can explain why there is a rather large difference between the activation energies of $CF_3CF_2OCF_2CF_3$ and CF_3OCF_3. Table 4 also shows that at the same level of theory and for the same compound, the activation energy for TS2 is approximately 20−30 kJ/mol lower than that of TS1 and the prefactor K_0 is approximately 2−8 times higher than that of TS1.

4. Conclusions

The effect of AlF_3 on the decomposition of CF_3OCF_3 and $CF_3CF_2OCF_2CF_3$ is investigated by ab initio theory. Previous work by Pancansky et al.[7] showed that AlF_3 significantly reduces the activation energy of the decomposition of CF_3OCF_3 due to the strong electrostatic interaction between the aluminum trifluoride and the reactant. In this work, a new transition-state structure and reaction mechanism have been proposed to describe the decomposition of CF_3OCF_3 in the presence of AlF_3. This new mechanism shows that AlF_3 functions by accepting a fluorine atom from one carbon and simultaneously donating a fluorine atom to the other carbon. We show that the same reaction pathway is obtained independently of the level of theory, using both B3lYP 6-31G* and B3LYP 6-311G*. The reaction rate, generated via statistical mechanics and transition-state theory, is 2−3 orders of magnitude higher for the new transition state as compared to that of the old transition state. The study was also performed for $CF_3CF_2OCF_2CF_3$ in order to ascertain the effect of chain length on the reaction mechanism and rate. We found that an analogous transition state with a lower activation energy provides the lowest-energy path for decomposition of the longer chain. In the presence of AlF_3, the reaction rate of $CF_3CF_2OCF_2CF_3$ is generally 2−3 orders higher than that of CF_3OCF_3.

Acknowledgment. This work was supported by the Air Force Office of Scientific Research through Contract #AF FA 9550-05-1-0342. We also greatly appreciated the comments and corrections of an anonymous reviewer for great improvement.

Supporting Information Available: Optimized angles and dihedrals and coordinates of major compounds. This material is available free of charge via the Internet at http://pubs.acs.org.

References and Notes

(1) Snyder, C. E.; Jr.; Gschwender, L. J.; Scott, O. L. *Tribol. Trans.* **1995**, *38*, 733.
(2) Tanaka, Y.; Nojiri, N.; Ohta, K.; Kubota, H.; Makita, T. *Int. J. Thermophys.* **1989**, *10*, 857.
(3) Bell, G. A.; Howell, J.; Del Pesco, T. W. Perfluoroalkylpolyethers. In *Synthetic Lubricants and High-Performance Functional Fluids*; Rudnick, L. R., Shubkin, R. L., Eds.; Marcel Dekker, Inc: New York, 1999; p 215.
(4) Pacansky, J.; Waltman, R. J.; Jebens, D.; Heery, O. *J. Fluorine Chem.* **1997**, *82*, 85.
(5) Gschwender, L. J.; Sharma, S. K.; Snyder, C. E.; Jr.; Helmick, L.; Fultz, G. W.; Bruce, S. *Tribol. Trans.* **1998**, *41*, 78.
(6) Li, P.; Lyth, E.; Mumro, D.; Ng, L. M. *Tribol. Lett.* **1998**, *4*, 109.
(7) Pacansky, J.; Waltman, R. J. *J. Fluorine Chem.* **1997**, *83*, 41.
(8) Pacansky, J.; Waltman, R. J. *J. Fluorine Chem.* **1997**, *82*, 79.
(9) Waltman, R. J. *J. Fluorine Chem.* **1998**, *90*, 9.
(10) Parr, R. G.; Yang, W. *Density-Functional Theory of Atoms and Molecules*; Oxford University Press: New York, 1989.
(11) Becke, A. D. *J. Chem. Phys.* **1992**, *96*, 2155.
(12) Becke, A. D. *J. Chem. Phys.* **1992**, *97*, 9173.
(13) Becke, A. D. *J. Chem. Phys.* **1993**, *98*, 5648.
(14) Lee, C.; Yang, W.; Parr, R. G. *Phys. Rev. B* **1988**, *37*, 785.
(15) Raghavachari, K.; Pople, J. A. *Int. J. Quantum Chem.* **1981**, *20*, 1067.
(16) Frisch, M. J.; Trucks, G. W.; Schlegel, H. B.; Scuseria, G. E.; Robb, M. A.; Cheeseman, J. R.; Zakrzewski, V. G.; Montgomery, J. A., Jr.; Stratmann, R. E.; Burant, J. C.; Dapprich, S.; Millam, J. M.; Daniels, A. D.; Kudin, K. N.; Strain, M. C.; Farkas, O.; Tomasi, J.; Barone, V.; Cossi, M.; Cammi, R.; Mennucci, B.; Pomelli, C.; Adamo, C.; Clifford, S.; Ochterski, J.; Petersson, G. A.; Ayala, P. Y.; Cui, Q.; Morokuma, K.; Malick, D. K.; Rabuck, A. D.; Raghavachari, K.; Foresman, J. B.; Cioslowski, J.; Ortiz, J. V.; Stefanov, B. B.; Liu, G.; Liashenko, A.; Piskorz, P.; Komaromi, I.; Gomperts, R.; Martin, R. L.; Fox, D. J.; Keith, T.; Al-Laham, M. A.; Peng, C. Y.; Nanayakkara, A.; Gonzalez, C.; Challacombe, M.; Gill, P. M. W.; Johnson, B. G.; Chen, W.; Wong, M. W.; Andres, J. L.; Head-Gordon, M.; Replogle, E. S.; Pople, J. A. *Gaussian 98*; Gaussian, Inc.: Pittsburgh, PA, 1998.
(17) Horn, H.; Lengsfield, B. H.; Rice, J. E.; Mclean, A. D.; Carter, J. T.; Replogle, E. S.; Barnes, L. A.; Maluends, S. A.; Lie, G. C.; Gutowski, M.; Rudge, W. E.; Sauer, S. P. A.; Lindh, R.; Andersson, K.; Chevalier, T. S.; Widmark, P. O.; Bouzida, D.; Pacansky, G.; Singh, K.; Gillan, C. J.; Carnervali, P.; Swope, W. C.; Liu, B. *Mulliken 2.0*; Almaden Research Center, IBM Research Division: San Jose, CA, 1996.
(18) Glasstone, S.; Laidler, K. J.; Eyring, H. *The Theory of Rate Process*; McGraw-Hill: New York, 1941.
(19) McQuarrie, D. A. *Statistical Mechanics*; University Science Books: Sausalito, CA, 2000.
(20) Leininger, J.-P.; Minot, C.; Lorant, F.; Francoise, B. *J. Phys. Chem. A* **2007**, *111*, 3082.
(21) Foresman, J. B.; Frisch, A. J. *Exploring Chemistry with Electronic Structure Methods*; Gaussian, Inc: Pittsburgh, PA, 1993.
(22) Scott, A. P.; Radom, L. *J. Phys. Chem.* **1996**, *100*, 345.
(23) Bauschlicher, C. W. J.; Partridge, H. *J. Chem. Phys.* **1995**, *103*, 1788.
(24) Pitzer, K. S.; Gwinn, W. D. *J. Chem. Phys.* **1942**, *10*, 428.
(25) Hase, W. L. *Acc. Chem. Res.* **1983**, *16*, 258.

(26) Li, H.-C. Ph.D. Dissertation, University of Tennessee, Knoxville, TN, 2001.
(27) Li, H.-C.; McCabe, C.; Cui, S. T.; Cummings, P. T.; Cochran, H. D. *Mol. Phys.* **2002**, *100*, 265.
(28) Li, H.-C.; McCabe, C.; Cui, S. T.; Cummings, P. T.; Cochran, H. D. *Mol. Phys.* **2003**, *101*, 2157.
(29) Jiang, B.; Crawford, N. J.; Keffer, D. J.; Edwards, B. J.; Adcock, J. L. *Mol. Simul.* **2007**, *33*, 881.